cmgh
CELLULAR AND MOLECULAR GASTROENTEROLOGY AND HEPATOLOGY

ORIGINAL RESEARCH

Regulation of Gastric Lgr5+ve Cell Homeostasis by Bone Morphogenetic Protein (BMP) Signaling and Inflammatory Stimuli

Wei Ye,[1,2,*] Hidehiko Takabayashi,[1,*] Yitian Yang,[1,2] Maria Mao,[1] Elise S. Hibdon,[3] Linda C. Samuelson,[3] Kathryn A. Eaton,[4] and Andrea Todisco[1]

[1]Department of Internal Medicine, [3]Department of Molecular and Integrative Physiology, [4]Department of Microbiology and Immunology, University of Michigan Medical Center, Ann Arbor, Michigan; [2]Department of Gastroenterology, Hangzhou Chinese Medicine Hospital, Hangzhou, Zhejiang, China

SUMMARY

This study reports the novel observation that inflammation and inhibition of bone morphogenetic protein signaling activate Leucine-rich repeat-containing G-protein-coupled receptor 5 +ve cells located on the lesser curvature of the oxyntic mucosa that give rise to spasmolytic polypeptide expressing metaplasia as well as dysplastic, proliferating lineages. These findings offer new insights into the mechanisms that lead to gastric metaplasia and dysplasia.

BACKGROUND & AIMS: Gastric Leucine-rich repeat-containing G-protein-coupled receptor 5 (Lgr5) cells exert important functions during injury and homeostasis. Bone morphogenetic protein (BMP) signaling regulates gastric inflammation and epithelial homeostasis. We investigated if BMP signaling controls the fate of Lgr5^{+ve} cells during inflammation.

METHODS: The *H^+/K^+-adenosine triphosphatase β-subunit* promoter was used to express the BMP inhibitor noggin (*Nog*) in the stomach (*H^+/K^+-Nog* mice). Inhibition of BMP signaling in Lgr5 cells was achieved by crossing *Lgr5-EGFP-ires-CreERT2* (*Lgr5-Cre*) mice to mice with floxed alleles of BMP receptor 1A (*Lgr5-Cre;Bmpr1a$^{flox/flox}$* mice). Lgr5/GFP^{+ve} cells were isolated using flow cytometry. Lineage tracing studies were conducted by crossing *Lgr5-Cre* mice to mice that express *Nog* and *tdTomato* (*Lgr5-Cre;H^+/K^+-Nog;Rosa26-tdTom*). Infection with *Helicobacter felis* was used to induce inflammation. Morphology of the mucosa was analyzed by H&E staining. Distribution of H^+/K^+-adenosine triphosphatase-, IF-, Ki67-, CD44-, CD44v9-, and bromodeoxyuridine-positive cells was analyzed by immunostaining. Expression of neck and pit cell mucins was determined by staining with the lectins Griffonia (Bandeiraea) simplicifolia lectin II and Ulex europaeus agglutinin 1, respectively. *Id1*, *Bmpr1a*, *Lgr5*, *c-Myc*, and *Cd44* messenger RNAs were measured by quantitative reverse-transcription polymerase chain reaction.

RESULTS: *Lgr5-Cre;Bmpr1a$^{flox/flox}$* mice showed diminished expression of *Bmpr1a* in Lgr5/GFP^{+ve} cells. Infection of *Lgr5-Cre;Bmpr1a$^{flox/flox}$* mice with *H felis* led to enhanced inflammation, increased cell proliferation, parietal cell loss, and to the development of metaplasia and dysplasia. Infected *Lgr5-Cre;H^+/K^+-Nog;Rosa26-tdTom* mice, but not control mice, showed the presence of tomato^{+ve} glands lining the lesser curvature that stained positively with Griffonia (Bandeiraea) simplicifolia lectin II and Ulex europaeus agglutinin 1, and with anti-IF, -CD44, -CD44v9, and -bromodeoxyuridine antibodies.

CONCLUSIONS: Inflammation and inhibition of BMP signaling activate Lgr5^{+ve} cells, which give rise to metaplastic, dysplastic, proliferating lineages that express markers of mucus neck and zymogenic cell differentiation. *(Cell Mol Gastroenterol Hepatol 2018;5:523–538; https://doi.org/10.1016/j.jcmgh.2018.01.007)*

Keywords: Chief Cells; Dysplasia; Differentiation; Metaplasia.

Chronic inflammation has been recognized as an important causative factor for the development of gastric metaplasia, dysplasia, and neoplasia. Numerous experimental models have confirmed that exposure of the gastric epithelium to chronic inflammatory stimuli such as infection with *Helicobacter* organisms can lead to significant aberrations in gastric epithelial homeostasis.[1–5]

The mechanisms involved in the pathogenesis of metaplasia, dysplasia, and neoplasia in the context of chronic inflammation have been only partially characterized. One current hypothesis is that chronic inflammation and mucosal injury can cause aberrations in the normal biological functions of gastric epithelial cells, leading to the development of metaplastic and dysplastic changes of the gastric mucosa and, ultimately, to neoplasias.[1–6] Indeed, both intestinal metaplasia and spasmolytic polypeptide expressing

*Authors share co-first authorship.

Abbreviations used in this paper: **ATPase, adenosine triphosphatase; BMP, bone morphogenetic protein; BrdU, bromodeoxyuridine; EGFP, enhanced green fluorescent protein; ERK, extracellular signal–regulated kinase; GFP, green fluorescent protein; GSII, Griffonia (Bandeiraea) simplicifolia lectin II; HBSS, Hank's balanced salt solution; H/K-nog, H/K-noggin; IF, intrinsic factor; mRNA, messenger RNA; QRT-PCR, quantitative reverse-transcription polymerase chain reaction; SPEM, spasmolytic polypeptide expressing metaplasia; TFF2, Trefoil factor 2.**

Most current article

2352-345X
https://doi.org/10.1016/j.jcmgh.2018.01.007

metaplasia (SPEM), which is characterized by the aberrant expression of Trefoil factor 2 (TFF2), and of mucins that bind the lectin Griffonia (Bandeiraea) simplicifolia lectin II (GSII) at the base of glands of the oxyntic mucosa, have been associated with inflammation-induced gastric neoplasms.[2,5,7–9] It has been suggested that SPEM might derive from reprograming of zymogenic cells during situations of inflammation and injury such as those triggered by infection with *Helicobacters*.[10]

Several studies have identified, on the basis of expression of molecular markers, such as the Wnt target gene *Lgr5*,[11] populations of gastric epithelial cells that can self-renew and that can show multilineage differentiation capacity. In addition to *Lgr5*, other potential markers for gastric stem/progenitor cells have been investigated recently, including *villin*, *Prom1/Cd133*, *Cd44*, *Dckl1/ Dcamkl1*, *Troy*, *Mist-1, Sox-2*, *Tff2*, and *Runx1*.[11–17] It has been suggested that genetic and epigenetic alterations of these cells might lead to their transformation and to the initiation of tumor growth.[14]

Leucine-rich repeat-containing G-protein-coupled receptor 5 (Lgr5) cells, in particular, have been shown to play an important role in gastrointestinal tissue homeostasis.[11,13,14] In the stomach, cells with *Lgr5* transcriptional activity initially were identified at the base of antral glands and, to a lesser degree, along the lesser curvature of the oxyntic mucosa, an area known to be one of the most common locations for the development of gastric carcinomas.[11,18,19] Recent studies, however, which have taken advantage of a different mouse model, have shown that Lgr5 cells are widely distributed in glands of the corpus where they represent a subpopulation of chief cells.[20] It also has been suggested that in the corpus these cells do not show stem cell characteristics during homeostasis but that after injury they acquire stem cell functions to promote epithelial repair.[20]

An increased number of *Lgr5*-expressing cells has been detected in patients with gastritis and intestinal metaplasia and in gastric carcinomas.[20–22] In support of these findings, a recent study showed that *Lgr5*-expressing chief cells can be a major cell-of origin of gastric neoplasms.[20] Reports also have shown that inflammatory stimuli such as *Helicobacter* organisms can adhere to *Lgr5*-expressing cells, leading to their proliferation and activation.[23]

The bone morphogenetic proteins (BMPs) are regulatory peptides that exert important effects on the growth and differentiation of gastrointestinal tissues. The actions of these proteins can be blocked by secreted inhibitory molecules, such as noggin, gremlin, and chordin, which are expressed in vivo to modulate the actions of the BMPs.[24,25] It has been shown that loss of BMP signaling in the stomach leads to perturbations of the normal homeostatic mechanisms of the gastric mucosa, leading to the development of metaplasia, dysplasia, and neoplasia.[25–27] In support of these observations studies have shown that BMP receptors such as BMPR1A and the BMP signal transducing proteins Smad1, 5, and 8 are widely expressed in the glandular stomach.[26,28]

In a series of published studies[26] we showed that transgenic expression in the corpus of the mouse stomach of the BMP inhibitor *noggin* leads to the development of SPEM, parietal cell loss, and to increased cell proliferation. We also reported that expression of noggin enhances *H felis*– *and Helicobacter pylori*–induced inflammation and gastric epithelial cell proliferation, leading to the accelerated development of dysplasia, and to increased expression and activation of the oncogenic proteins activation-induced cytidine deaminase and signal transducer and activator of transcription (STAT)3.[27]

The mechanisms that regulate the number and function of $Lgr5^{+ve}$ cells during gastric inflammation, and those involved in the development of gastric metaplasia and dysplasia, have been only partially characterized. Accordingly, we sought to investigate the role of BMP signaling in the regulation of Lgr5 cell homeostasis during gastric inflammation. In particular, we tested the hypothesis that inflammation and inhibition/ loss of BMP signaling induce the activation of $Lgr5^{+ve}$ cells, located in the oxyntic mucosa of the lesser curvature, that lead to the development of metaplastic and dysplastic epithelial cell lineages.

Materials and Methods

Mice

The *H/K-noggin* (*H/K-nog*) transgenic mice were generated in our laboratory and they were described previously.[26] Pathogen-free C57BL/6 mice, *Lgr5-enhanced green fluorescent protein (EGFP)-ires-CreERT2* (*Lgr5-Cre*) mice, in which the expression of both *Cre* and green fluorescent protein (*GFP*) is driven by endogenous *Lgr5* regulatory sequences,[11] and *Rosa26-tdTom* (*Rosa26-Tom*) mice aged 4–10 weeks were purchased from Jackson Laboratory (Bar Harbor, ME). $Bmpr1a^{flox/flox}$[29] mice were received from the laboratory of Dr Yuji Mishina (University of Michigan). Mouse genotyping was described elsewhere.[26]

Specific inhibition of BMP signaling in Lgr5 cells was achieved by crossing *Lgr5-Cre* mice to $Bmpr1a^{flox-flox}$ mice to generate *Lgr5-Cre;*$Bmpr1a^{flox-flox}$ mice. To conduct lineage tracing in the presence of Noggin, H^+/K^+*-nog* mice were crossed to *Rosa26-Tom* reporter mice to generate H^+/K^+*-nog;Rosa26-Tom* mice. *Lgr5-Cre* mice then were crossed to both H^+/K^+*-Nog;Rosa26-Tom* and *Rosa26-Tom* mice to generate *Lgr5-Cre;*H^+/K^+*-Nog;Rosa26-Tom* and *Lgr5-Cre;Rosa26-Tom* mice. Cre was activated by 1 intraperitoneal injection of tamoxifen (0.1 mg/g body weight). All mice, including *Lgr5-Cre*, *Lgr5-Cre;*$Bmpr1a^{flox-flox}$, *Lgr5-Cre;*H^+/K^+*-Nog;Rosa26-Tom*, and *Lgr5-Cre;Rosa26-Tom* mice received tamoxifen injections. The mice were maintained on a C57BL/6 background. In some experiments, mice were injected with 200 μL of a 10 mg/mL solution of bromodeoxyuridine (BrdU, BD Biosciences, San Jose, CA) 2 hours before tissue collection. In all experiments, animals were fasted overnight with free access to water before tissue collection. Mice were housed under specific pathogen-free conditions in automated watered and ventilated cages on a 12-hour light/ dark cycle in the animal maintenance facility at the University of Michigan. All animal experiments were approved by the University of Michigan Animal Care and Use Committee.

H felis *Culture and Infection*

Two- to 3-month-old *Lgr5-Cre* mice, *Lgr5-Cre;*$Bmpr1a^{flox/flox}$mice, *Lgr5-Cre;Rosa26-Tom* mice, and

Lgr5-Cre;H^{+}*/K*$^{+}$*-Nog;Rosa26-Tom* mice were inoculated orally with overnight broth cultures of approximately 10^8 cfu of *H felis* organisms.[27,30] Control animals were inoculated with broth without organisms. Both infected and noninfected animals were killed 12 weeks after inoculation. Similar numbers of male and female mice were used for the studies.

RNA Isolation and Quantitative Reverse-Transcription Polymerase Chain Reaction Analysis

RNA was isolated from full-thickness samples of the corpus of mice using TRIzol reagent (Invitrogen, Carlsbad, CA), followed by DNase treatment and purification with the RNeasy Mini kit (Qiagen, Valencia, CA).[26] Quantitative reverse-transcription polymerase chain reaction (QRT-PCR) was performed according to previously published methods[26] using primer sequences and protocols that were obtained from commercially available sources. *Gapdh*, *Cd44*, and *Bmpr1a* primers were obtained from Integrated DNA Technologies (Coralville, IA). *Bmpr1a* QRT-PCR primers span exons 2–3 of the gene. The sequences are as follows: primer 5'-CTTGGCAATGACTTTCACCTG-3' binds in exon 3 (284-304 in Genebank NM-009758.4), primer 5'-TCGCTTTGA TACTGTCTTGGAA-3' binds in exon 2 (170-191 in Genebank NM-009758.4). The deletion in the *Bmpr1a* floxed mice from the laboratory of Y. Mishina deletes a portion of exon 2. Accordingly, these primers will not amplify a product in the recombined mice. The *Id1*, *c-Myc*, and *Lgr5* primers were obtained from Qiagen.

Gastric Epithelial Cell Isolation and Flow Cytometry

Fluorescence-activated cell sorting isolation of Lgr5/GFP^{+} cells from *Lgr5-Cre* and *Lgr5-Cre;Bmpr1a*$^{flox/flox}$

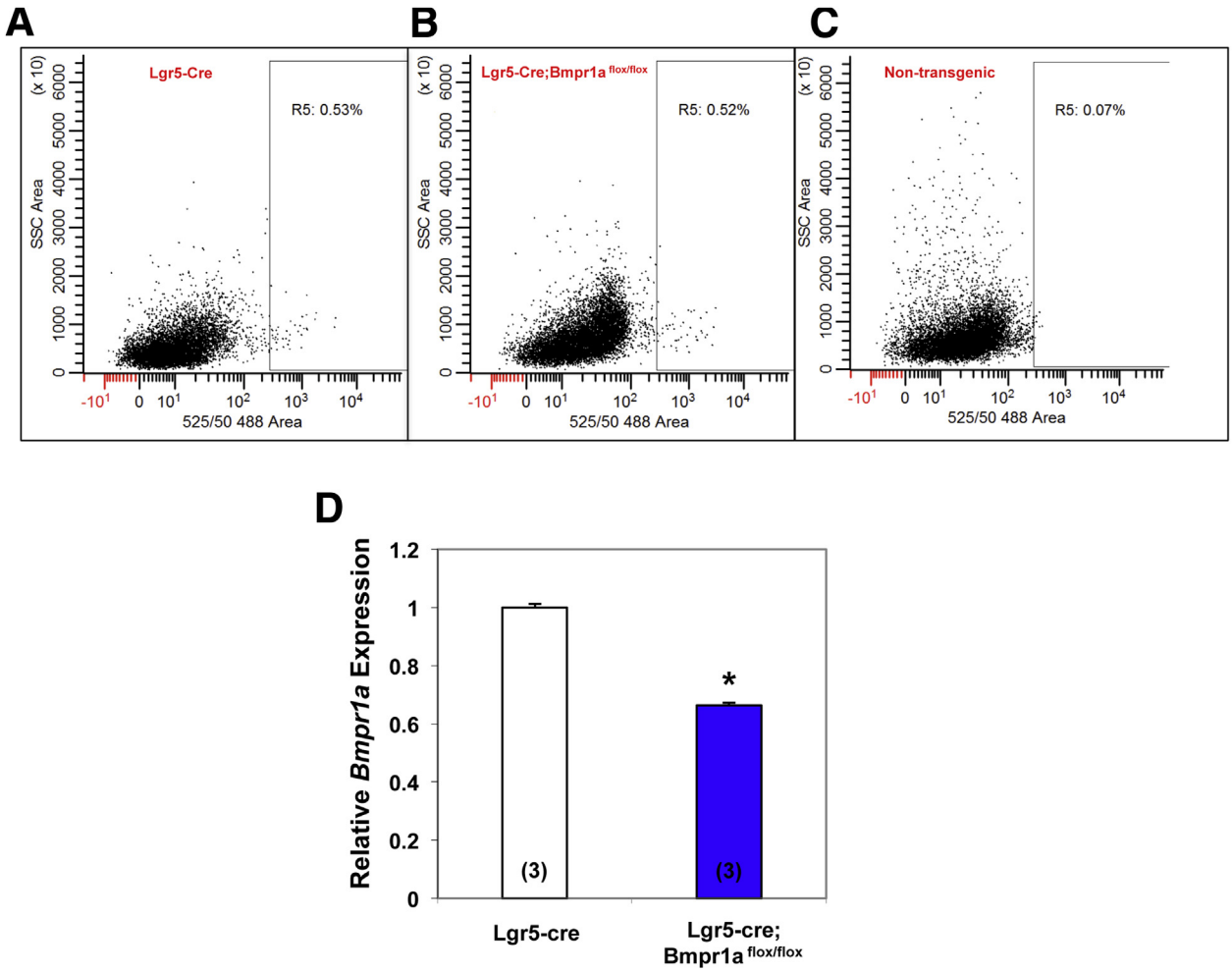

Figure 1. Deletion of *Bmpr1a* in Lgr5 cells. GFP^{+ve} cells from 1- to 2-month-old *Lgr5-EGFP-ires-CreERT2* mice (*Lgr5-Cre* mice) and *Lgr5-EGFP-ires-CreERT2;Bmpr1a*$^{flox-flox}$ mice (*Lgr5-Cre;Bmpr1a*$^{flox-flox}$ mice) were isolated by flow cytometry. Mice were treated with 1 intraperitoneal. injection of tamoxifen (0.1 mg/g body weight) and killed 15 days after tamoxifen. Flow cytometry plots of cells isolated from (*A*) *Lgr5-Cre* mice and (*B*) *Lgr5-Cre;Bmpr1a*$^{flox-flox}$ mice. (*C*) Flow cytometry plot of cells isolated from nontransgenic negative control mice. (*D*) *Bmpr1a* mRNA signals in cells from *Lgr5-Cre;Bmpr1a*$^{flox-flox}$ mice were compared with those detected in cells from control mice using QRT-PCR. Values are shown as means ± SE. Numbers in parenthesis indicate the number of animals used in each group. *$P < .05$.

mice was performed as previously described,[31] with modifications. Both *Lgr5-Cre* and *Lgr5-Cre;Bmpr1a*$^{flox/flox}$ mice were injected with 1 intraperitoneal injection of tamoxifen (0.1 mg/g body weight). The mice were killed 15 days after tamoxifen injection. Samples of gastric mucosa were placed in Mg^{2+}-, Ca^{2+}-free Hank's balanced salt solution (HBSS), 5% fetal bovine serum, 2 mmol/L EDTA, shaken for 20 minutes at 37°C, and filtered through a 100-μm cell strainer. After filtration the samples were pelleted and resuspended in HBSS containing 0.1 U/mL Liberase (Roche, Basel, Switzerland) and 40 μg/mL DNase I (Sigma, St. Louis, MO). The solutions were shaken for 10 minutes at 37°C, filtered through a 100-μm cell strainer, and spun at 1500 rpm for 5 minutes. After 1 wash with HBSS, the pellets were resuspended in HBSS containing aqua viability dye (Live/Dead Fixable Aqua dead cell stain kit; Invitrogen) according to the manufacturer's instructions. After 1 wash the cells were resuspended in HBSS containing 1% fetal bovine serum, filtered through a 50-μm filter (Partec/Sysmex, Lincolnshire, IL), and used for analysis. GFP^{+ve} cells were isolated using fluorescence-activated cell sorting. Analyses were performed using an iCyte Synergy (Sony Biotechnology, San Jose, CA) with WINLIST V.8 software (VertySoftware House, available: http://www.vsh.com). The laser emission wavelengths and filter used were 488-nm laser with a 525/50-nm filter. Aqua viability dye was excited with a 405-nm laser and detected with a 577/25-nm filter. The sorted cells were collected into sterile 1.5-mL tubes containing 300 μL RNA lysis buffer and used for RNA extraction (Zymo Research, Irvine, CA).

Histochemical Analysis and Image Acquisition

Tissue fixation, generation of paraffin sections, H&E staining, and immunostaining were performed according to previously published methods.[26,27] Sections were stained with the following primary antibodies: anti-H^+/K^+-adenosine triphosphatase (ATPase) α-subunit (1:500, catalog number: DO31-3; Medical and Biological Laboratories, Nagoya, Japan), anti-Ki67 (1:500, catalog number: MA5-14520; Thermo Scientific, Waltham, MA), anti-BrdU (1:200, catalog number: MO744; Dako Corporation, Carpinteria, CA), anti-intrinsic factor (anti-IF) (1:1000; gift from Dr Jason Mills, Washington University, St. Louis, MO), anti-red fluorescent protein (1:200, catalog number: 600-401-379; Rockland/Biomol, Hamburg, Germany), anti-TFF2 (1:200, catalog number: ab49536; Abcam, Cambridge, UK), anti-CD44 (1:30, catalog number: 550538; BD Biosciences), anti-CD44v9 (1:200, catalog number CAC-LKG-M002; Cosmo Bio, Carlsbad, CA), and with Alexa 488–conjugated anti-GFP (1:200, catalog number A21311; Invitrogen). In some experiments the slides were stained for 1.5 hours at 37°C with Alexa 488–conjugated GSII (1:1000, catalog number: FL-1211; Vector Laboratories, Burlingame, CA) and fluorescein isothiocyanate–conjugated Ulex europaeus agglutinin 1 lectin (1:200, catalog number: FL-1061; Vector Laboratories). For immunohistochemistry with

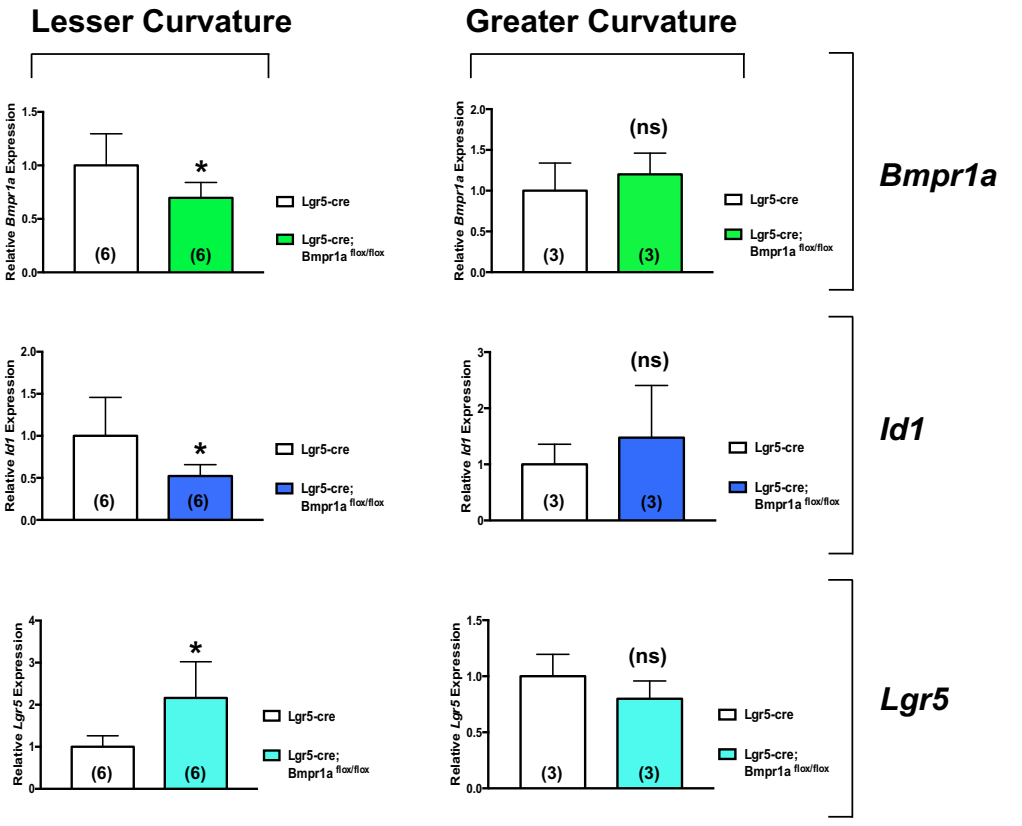

Figure 2. Expression of *Bmpr1a*, *Id1*, and *Lgr5* in the lesser and greater curvatures of *Lgr5-Cre* and *Lgr5-Cre;Bmpr1a*$^{flox-flox}$ mice. One- to 2-month-old *Lgr5-Cre* mice and *Lgr5-Cre;Bmpr1a*$^{flox-flox}$ mice were treated with 1 intraperitoneal injection of tamoxifen (0.1 mg/g body weight) and killed 5 months after tamoxifen. *Bmpr1a*, *Id1*, and *Lgr5* mRNA signals in the lesser and greater curvatures of *Lgr5-Cre* mice were compared with those detected in *Lgr5-Cre;Bmpr1a*$^{flox-flox}$ mice using QRT-PCR. Values are shown as means ± SE. Numbers in parenthesis indicate the number of animals used in each group. *$P < .05$.

detection with diaminobenzidine as substrate, slides were rinsed and subsequently treated with biotin-conjugated secondary antibodies (1:200; Vector Laboratories) for 30 minutes at room temperature. To visualize biotin staining, the Vectastain Elite ABC kit was used (Vector Laboratories). For immunofluorescence analysis, Alexa 555–donkey anti-rabbit (1:500), Alexa 594–donkey anti-rat (1:500), and Alexa 488–donkey anti-rat and anti-mouse (1:500) secondary antibodies were used (Molecular Probes, Eugene, OR). ProLong Gold Antifade reagent with 4′,6-diamidino-2-phenylindole (Invitrogen) was used for nuclear counterstain and mounting medium. Control experiments were performed by incubating the slides in the presence of the secondary antibodies without the primary antibodies (data not shown). Visualization of slides was performed with a Nikon (Tokyo, Japan) Eclipse E 800 fluorescence microscope for all other studies.

For histologic scoring of gastritis, sections from the stomachs of 3–4 separate animals from each of the 4 treatment groups were examined and scored largely as previously described.[32] Slides containing sections of well-oriented gastric glandular mucosa were examined in a blinded fashion. Only fields that contained full-thickness gastric mucosa that was oriented perpendicularly were analyzed. All well-oriented fields were scored. Each field was scored separately for the presence or absence and severity of neutrophilic cell infiltration, gastritis, and epithelial metaplasia/dysplasia.[32] The severity of the changes was graded using a scale from 1 (mild) to 3 (severe), as follows. For neutrophilic infiltration: a score of 1 was defined as 2–3 clusters of neutrophils in the lamina propria, a score of 2 was defined as many clusters of neutrophils, and a score of 3 was defined as neutrophils present throughout the lamina propria. For gastritis: a score of 1 was defined as focal displacement of glands by inflammatory infiltrate, a score of 2 was defined as inflammatory infiltrate displacing less than 50% of glands in the field, and a score of 3 was defined as more than 50% of glands displaced by inflammatory infiltrate. For dysplasia: a score of 1 (epithelial metaplasia) was defined as loss of parietal cells with replacement by mucus-type cells or SPEM; a score of 2 (cellular dysplasia) was defined as anisocytosis/karyosis, loss of polarity, abnormal shape, and/or multiple epithelial layers;

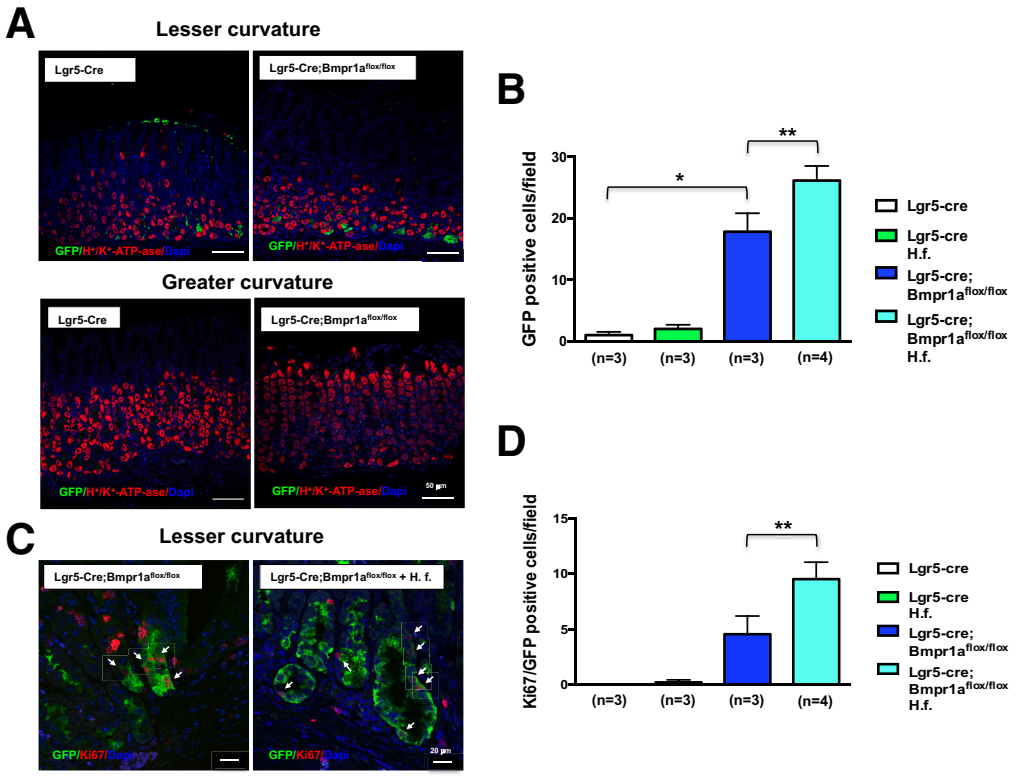

Figure 3. Regulation of cells with *Lgr5* transcriptional activity by BMP signaling. One- to 2-month-old *Lgr5-Cre* mice and *Lgr5-Cre;Bmpr1a*$^{flox\text{-}flox}$ mice were treated with 1 intraperitoneal injection of tamoxifen (0.1 mg/g body weight) and inoculated with *H felis* for 2 months after tamoxifen. Animals were analyzed 3 months after inoculation and 5 months after tamoxifen injection. (*A*) Paraffin sections of the lesser and greater curvatures of *Lgr5-Cre* and *Lgr5-Cre;Bmpr1a*$^{flox\text{-}flox}$ mice were stained with Alexa 488–conjugated anti-GFP antibodies (green) together with an anti-H^+,K^+-ATPase α-subunit primary antibody and an Alexa 555–conjugated secondary antibody (red). *Scale bar*: 50 μm. (*C*) Paraffin sections of the lesser curvature of *Lgr5-Cre* and *Lgr5-Cre;Bmpr1a*$^{flox\text{-}flox}$ mice were stained with Alexa 488–conjugated anti-GFP antibodies (green) together with an anti-Ki67 antibody and an Alexa 555–conjugated secondary antibody (red). *Scale bar*: 20 μm. *Arrows* point to GFP/Ki67-positive cells. *Bars* represent the number of (*B*) GFP- and of (*D*) GFP/Ki67-positive cells that were detected in the mucosa of the lesser curvature of *Lgr5-Cre* mice and of *Lgr5-Cre;Bmpr1a*$^{flox\text{-}flox}$ mice in the presence and absence of *H felis* (H. f.). Values are shown as means ± SE. Numbers in parenthesis indicate the number of animals used in each group. **P* < .05 vs *Lgr5-Cre* mice. ***P* < .05 vs *Lgr5-Cre;Bmpr1a*$^{flox\text{-}flox}$ mice. DAPI, 4'6-diamidino-2-phenylindole.

and a score of 3 (glandular dysplasia) was defined as dilation, irregularity, and disorganization of glands, with cellular dysplasia. Each field was scored, and the final score was calculated and expressed as a weighted average of all fields with that lesion as follows: sum of the number of fields for each score × the score, divided by the total number of fields.

The number of GFP-, H^+K^+-ATPase α-subunit– and Ki67-positive cells was determined by counting the number of stained cells in at least 3–4 fields in slides derived from 3 to 6 animals from each treatment group, using the Fiji imaging program (ImageJ, National Institutes of Health, Bethesda, MD).[33]

Data Analysis

Data are expressed as means ± SE. Statistical analysis was performed using the Student *t* test. *P* values less than .05 were considered significant.

Results

We sought to test the hypothesis that BMP signaling regulates the census and fate of Lgr5 cells in the oxyntic mucosa. Accordingly, we deleted BMP receptor 1A (*Bmpr1a*) in cells with *Lgr5* transcriptional activity. For these studies we took advantage of *Lgr5-Cre* mice, which express *Cre* and *EGFP* in cells with *Lgr5* transcriptional activity located only in glands of the antrum and of the lesser curvature, but not in those of the greater curvature.[11,18] To show diminished expression of *Bmpr1a* in Lgr5 cells from *Lgr5-Cre;Bmpr1a*$^{flox\text{-}flox}$ mice, we isolated GFP^{+ve} cells from the gastric mucosa of both *Lgr5-Cre* and *Lgr5-Cre;Bmpr1a*$^{flox\text{-}flox}$ mice using flow cytometry. As shown in Figure 1, GFP^{+ve} cells from *Lgr5-Cre;Bmpr1a*$^{flox\text{-}flox}$ mice showed diminished expression of *Bmpr1a* messenger RNA (mRNA) when compared with cells isolated from control *Lgr5-Cre* mice.

The finding that inhibition of *Bmpr1a* mRNA expression in *Lgr5-Cre;Bmpr1a*$^{flox\text{-}flox}$ mice was not complete likely reflects variable levels of efficiency of *Cre*-mediated recombination in Lgr5 cells. It is conceivable that not all *Cre*-expressing Lgr5 cells could effectively and equally delete the target (*Bmpr1a*) after tamoxifen activation.

The specificity of this effect and the presence of effective inhibition of BMP signaling were confirmed by QRT-PCR assays that showed a significant decrease in the expression

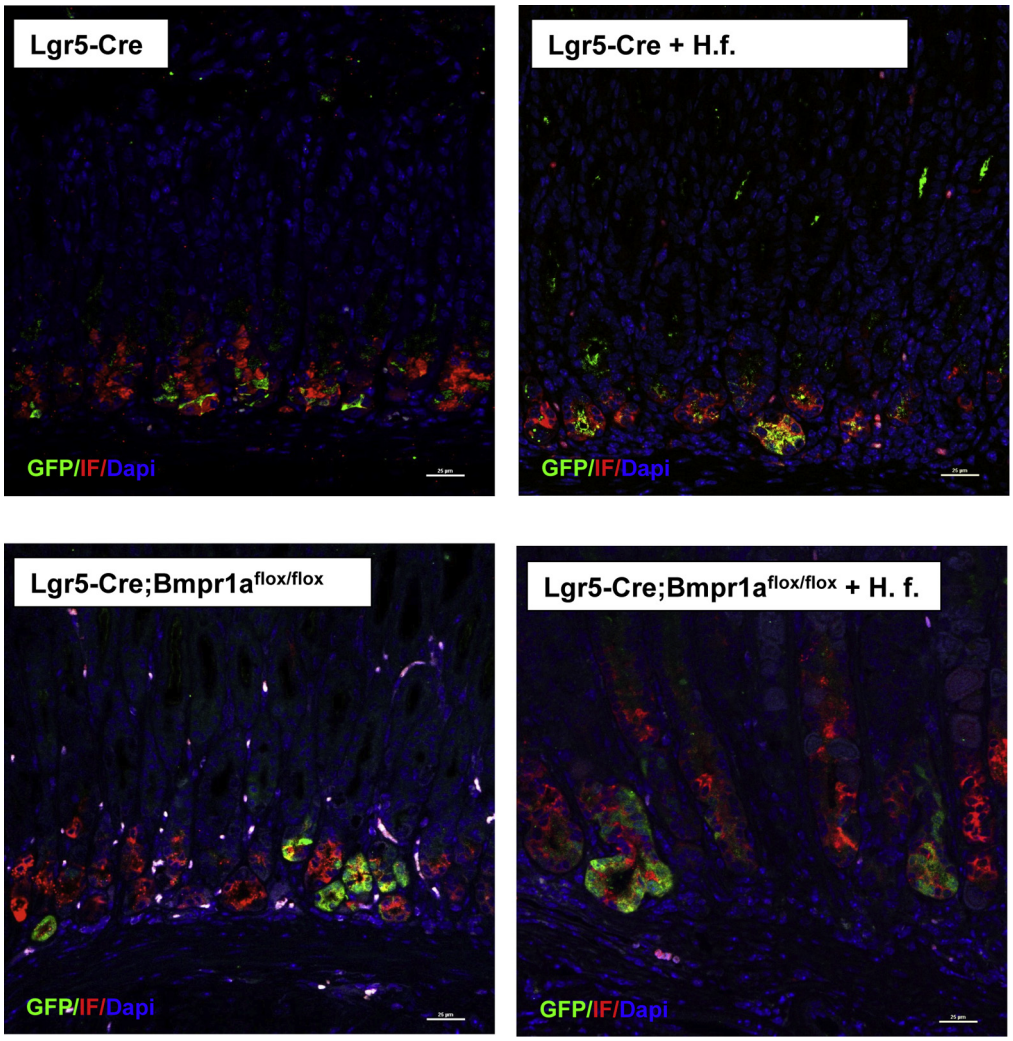

Figure 4. Expression of IF in cells with *Lgr5* transcriptional activity. One- to 2-month-old *Lgr5-Cre* mice and *Lgr5-Cre;Bmpr1a*$^{flox\text{-}flox}$ mice were treated with 1 intraperitoneal injection of tamoxifen (0.1 mg/g body weight) and inoculated with *H felis* 2 months after tamoxifen. Animals were analyzed 3 months after inoculation and 5 months after tamoxifen injection. Paraffin sections of the lesser curvature of *Lgr5-Cre* and of *Lgr5-Cre;Bmpr1a*$^{flox\text{-}flox}$ mice in the presence and absence of *H felis* (H. f.) were stained with anti-IF primary antibodies and an Alexa 555–conjugated secondary antibody (red) together with Alexa 488–conjugated anti-GFP antibodies (green). *Scale bar*: 25 μm. Similar results were observed in at least 1 other mouse and in 6 other mice in the *H felis*–infected *Lgr5-Cre;Bmpr1a*$^{flox\text{-}flox}$ group. DAPI, 4'6-diamidino-2-phenylindole.

of *Bmpr1a* and *Id1*, a well-characterized BMP-responsive gene,[34–36] together with an increase in that of *Lgr5* in samples obtained from the mucosa of the lesser, but not the greater curvature of *Lgr5-Cre;Bmpr1a*$^{flox\text{-}flox}$ mice (Figure 2).

We examined the distribution of cells with *Lgr5* transcriptional activity in the oxyntic mucosa of the lesser and greater curvatures of *Lgr5-Cre* mice.[11] Staining of sections of these areas of the stomach with anti-GFP and anti–H^+K^+-ATPase antibodies showed, in agreement with previously published reports,[11,18] that GFP^{+ve} cells are located in the mucosa of the lesser but not the greater curvature of *Lgr5-Cre;Bmpr1a*$^{flox\text{-}flox}$ mice (Figure 3*A*).

To investigate the role of BMP signaling in the regulation of Lgr5 cells during inflammation, we infected both *Lgr5-Cre* and *Lgr5-Cre;Bmpr1a*$^{flox\text{-}flox}$ mice with *H felis*, which is known to induce an inflammatory response in the gastric mucosa of mice.[37] The mice were studied 3 months after inoculation, and 5 months after tamoxifen injection. First, we examined if inhibition of BMP signaling in Lgr5 cells and the presence of *H felis* affect the number of cells with *Lgr5* transcriptional activity. Accordingly, we counted the number of GFP^{+ve} cells in sections obtained from the lesser curvature of both *Lgr5-Cre* and *Lgr5-Cre;Bmpr1a*$^{flox\text{-}flox}$ mice in the presence and absence of *H felis*. As shown in Figure 3*A* and *B*, *Lgr5-Cre;Bmpr1a*$^{flox\text{-}flox}$ mice showed a statistically significant increase in the number of GFP^{+ve} cells along the lesser but not the greater curvature. Infection with *H felis* further enhanced this effect (Figure 3*B* and *C*). We assessed if inhibition of BMP signaling and infection with *H felis* modulated the number of proliferating GFP^{+ve} cells. For these experiments we stained the sections with antibodies directed against both GFP and Ki67, a mitotic marker. As shown in Figures 3*C* and *D*, although both noninfected and *H felis*–infected *Lgr5-Cre* mice did not show the presence of a significant number of $Ki67^{+ve}/GFP^{+ve}$ cells, *Lgr5-Cre;Bmpr1a*$^{flox\text{-}flox}$ mice showed a significant increase in the number of proliferating GFP^{+ve} cells. The observation that this effect was more pronounced in the presence of *H felis* supports the notion that both BMP signaling and inflammatory stimuli regulate the census of $Lgr5^{+ve}$ cells.

A recent report has indicated that in the oxyntic mucosa Lgr5 cells represent a subset of chief cells.[20] Accordingly, we investigated if in our model, cells with *Lgr5* transcriptional activity express IF, a chief cell marker. Staining of sections of the lesser curvature of *Lgr-Cre* and *Lgr5-Cre;Bmpr1a*$^{flox\text{-}flox}$ mice in the presence or absence of *H felis*, with both

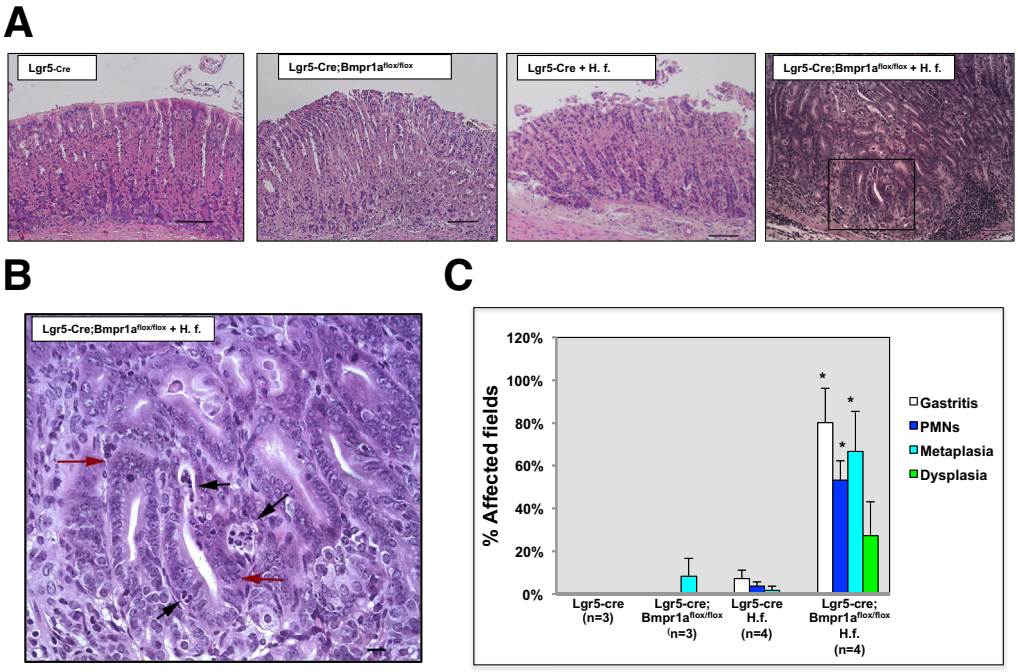

Figure 5. Enhanced inflammatory changes, metaplasia, and dysplasia in the gastric epithelium of *H felis*–infected *Lgr5-Cre;Bmpr1a*$^{flox\text{-}flox}$ mice. One- to 2-month-old *Lgr5-Cre* mice and *Lgr5-Cre;Bmpr1a*$^{flox\text{-}flox}$ mice were treated with 1 intraperitoneal injection of tamoxifen (0.1 mg/g body weight) and inoculated with *H felis* 2 months after tamoxifen. Animals were analyzed 3 months after inoculation and 5 months after tamoxifen injection. (*A*) Representative H&E-stained paraffin sections of the lesser curvature of *Lgr5-Cre* and of *Lgr5-Cre;Bmpr1a*$^{flox\text{-}flox}$ mice in the presence and absence of *H felis* (H. f.). The magnified window depicts dysplastic and inflammatory changes in *H felis*–infected *Lgr5-Cre;Bmpr1a*$^{flox\text{-}flox}$ mice. *Scale bars*: (*A*) 100 μm, (*B*) 25 μm. (*B*) *Red arrows* point to areas of dysplastic epithelium, *black arrows* indicate clusters of polymorphonuclear cells. (*C*) *Graph bars* represent the percentage of fields affected by gastritis, neutrophilic infiltrates, metaplasia, and dysplasia calculated in both *Lgr5-Cre* and *Lgr5-Cre;Bmpr1a*$^{flox\text{-}flox}$ mice in the presence and absence of *H felis*. Values are shown as means ± SE. Numbers in parenthesis indicate the number of animals used in each group. *$P < .05$ vs *H felis*–infected *Lgr5-Cre* mice.

anti-GFP and anti-IF antibodies, showed that chief cells express GFP, confirming the notion that Lgr5 cells represent a subpopulation of chief cells (Figure 4).

We examined the morphologic consequences of diminished expression of *Bmpr1a* in Lgr5 cells in the presence and absence of inflammatory stimuli. Microscopic and morphometric analysis of H&E-stained sections of the lesser curvature of uninfected *Lgr5-Cre* mice did not show any morphologic alterations, whereas infection with *H felis* induced only mild inflammation. In addition, uninfected *Lgr5-Cre;Bmpr1a*$^{flox\text{-}flox}$ mice showed the presence of minor metaplastic changes. In contrast, the mucosa of the lesser curvature of *H felis*–infected, *Lgr5-Cre;Bmpr1a*$^{flox\text{-}flox}$ mice showed robust morphologic abnormalities characterized by a reduction in the number of cells that had the morphologic appearance of parietal cells, a significant increase in the severity of the inflammatory infiltrates, and the presence of areas of metaplastic and dysplastic mucosa (Figure 5).

To confirm that inhibition of BMP signaling in Lgr5 cells and infection with *H felis* cause alterations in parietal cell homeostasis and induction of cell proliferation in the mucosa of the lesser curvature, we analyzed the number of parietal and proliferating cells by immunostaining for H^+,K^+-ATPase α-subunit and Ki67. As shown in the histologic sections and in the bar graphs shown in Figure 6 representing the number of positively stained cells, *H felis*–infected *Lgr5-Cre; Bmpr1a*$^{flox\text{-}flox}$ mice showed a marked decrease in the number of parietal cells (Figure 6*A* and *B*), and a robust increase in the number of Ki67-positive nuclei (Figure 6*C* and *D*). In contrast, uninfected *Bmpr1a*$^{flox\text{-}flox}$ mice showed only a mild decrease in parietal cell number and a small increase in the number of Ki67-positive cells. No significant changes were seen in both uninfected and infected control *Lgr5-cre* mice (Figure 6*B* and *D*).

We sought to investigate if infection with *H felis* and diminished expression of *Bmpr1a* in the gastric epithelium lead to the emergence of SPEM. For these studies we stained sections of the mucosa of the lesser curvature of both control noninfected and *H felis*–infected *Lgr5-Cre* and *Lgr5-Cre; Bmpr1a*$^{flox\text{-}flox}$ mice with specific anti-IF antibodies and with the lectin GSII, which is known to bind neck-cell mucins. As shown in the overlay images depicted in Figure 7, both infected and noninfected *Lgr5-Cre* mice did not show any significant abnormalities, whereas noninfected

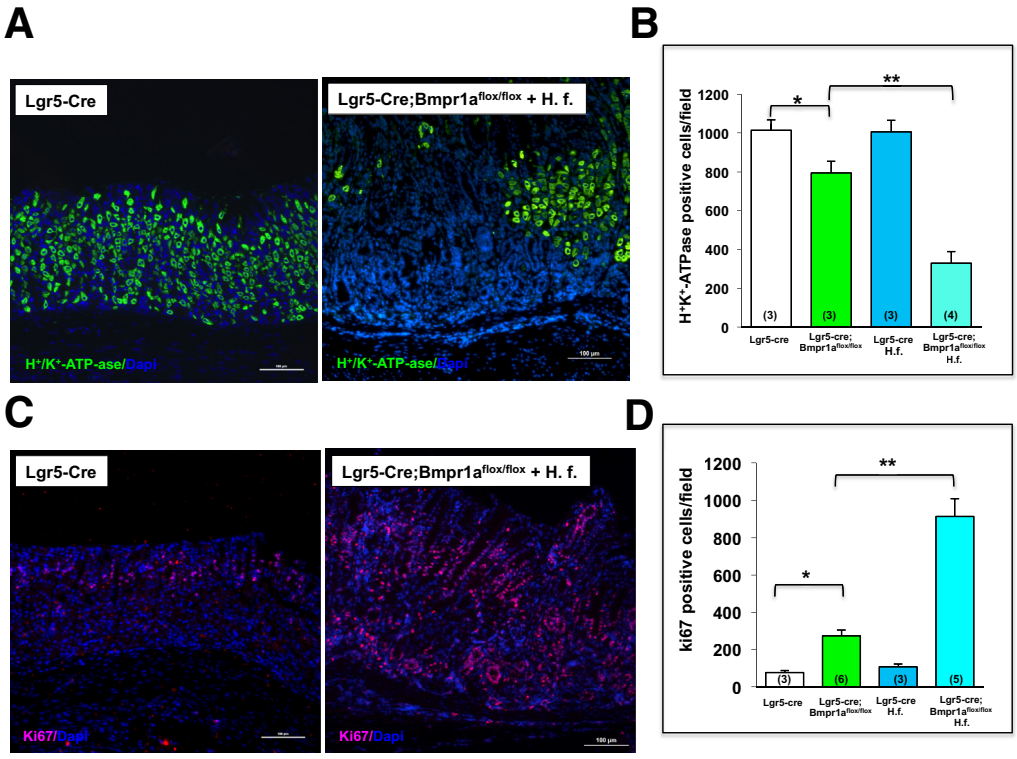

Figure 6. Decreased parietal cells and increased cell proliferation in *Helicobacter*-infected *Lgr5-Cre;Bmpr1a*$^{flox\text{-}flox}$ mice. One- to 2-month-old *Lgr5-Cre* mice and *Lgr5-Cre;Bmpr1a*$^{flox\text{-}flox}$ mice were treated with 1 intraperitoneal injection of tamoxifen (0.1 mg/g body weight) and inoculated with *H felis* 2 months after tamoxifen. Animals were analyzed 3 months after inoculation and 5 months after tamoxifen injection. Paraffin sections of the lesser curvature of *Lgr5-Cre* mice and of *Lgr5-Cre;Bmpr1a*$^{flox\text{-}flox}$ mice, in the presence and absence of *H felis* (H. f.), were stained with an (*A*) anti-H^+,K^+-ATPase α-subunit primary antibody and an Alexa 488–conjugated secondary antibody (green), and with an (*C*) anti-Ki67 primary antibody and an Alexa 555–conjugated secondary antibody (red). *Scale bars*: 100 μm. *Bars* represent the number of (*B*) H^+,K^+-ATPase α-subunit and of (*D*) Ki67-positive cells detected in *Lgr5-Cre* mice and in *Lgr5-Cre;Bmpr1a*$^{flox\text{-}flox}$ mice in the presence and absence of *H felis*. Values are shown as means ± SE. Numbers in parenthesis indicate the number of animals used in each group. *$P < .05$ vs *Lgr5-Cre* mice. **$P < .05$ vs *Lgr5-Cre;Bmpr1a*$^{flox\text{-}flox}$ mice. DAPI, 4'6-diamidino-2-phenylindole.

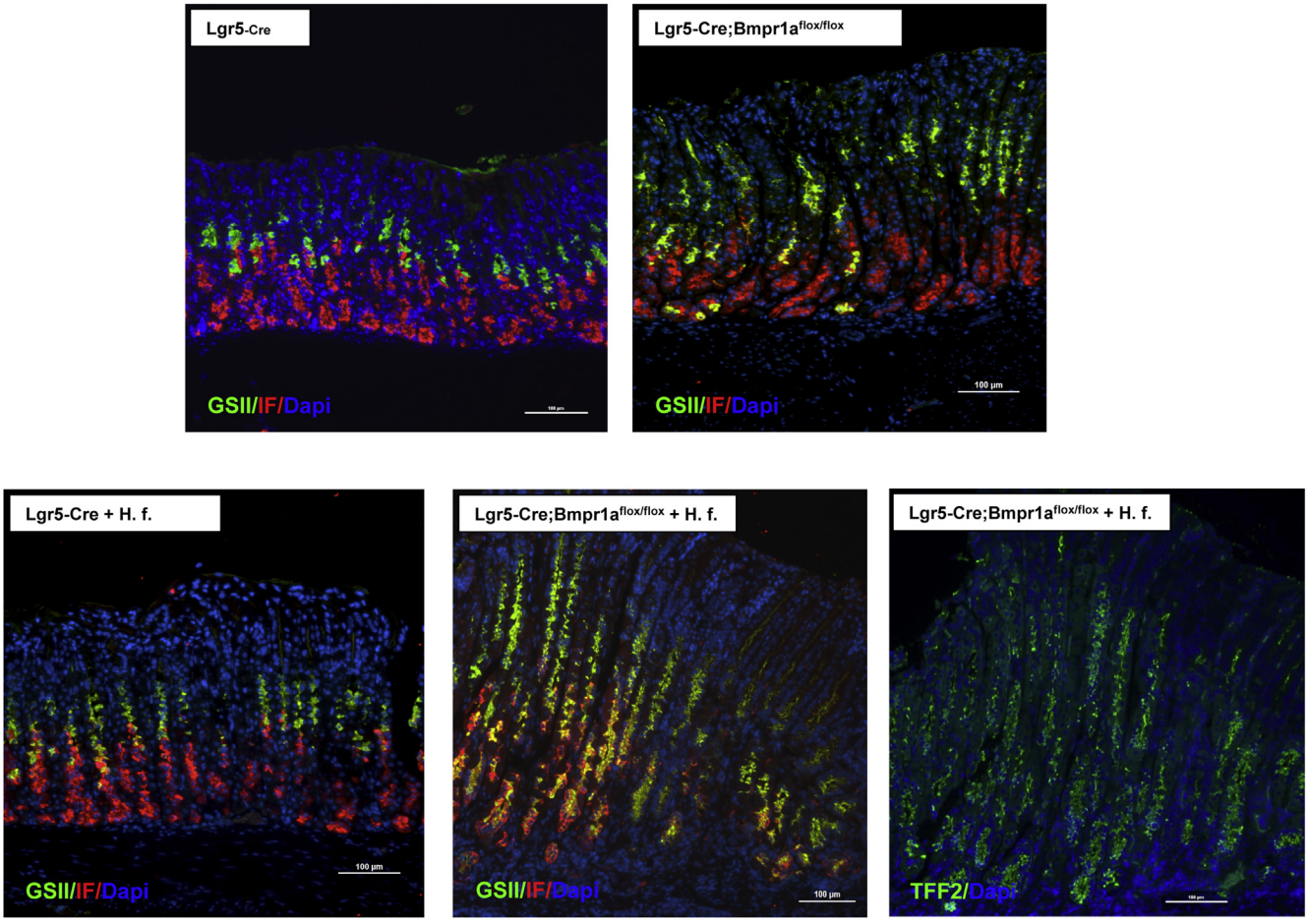

Figure 7. Development of SPEM in *H felis*–infected *Lgr5-Cre;Bmpr1a$^{flox-flox}$* mice. One- to 2-month-old *Lgr5-Cre* mice and *Lgr5-Cre;Bmpr1a$^{flox-flox}$* mice were treated with 1 intraperitoneal injection of tamoxifen (0.1 mg/g body weight) and inoculated with *H felis* 2 months after tamoxifen. Animals were analyzed 3 months after inoculation and 5 months after tamoxifen injection. Gastric paraffin sections of the lesser curvature of *Lgr5-Cre* and of *Lgr5-Cre;Bmpr1a$^{flox-flox}$* mice in the presence and absence of *H felis* (H. f.) were stained with anti-IF primary antibodies and Alexa 555–conjugated secondary antibodies (red) together with Alexa 488–conjugated GS II (green). Gastric paraffin sections of the lesser curvature of *H felis*–infected *Lgr5-Cre;Bmpr1a$^{flox-flox}$* mice were stained with anti-TFF2 primary antibodies and an Alexa 488–conjugated secondary antibody. *Scale bar*: 100 μm. Similar results were observed in at least 3 other mice in each group. DAPI, 4′,6-diamidino-2-phenylindole.

Lgr5-Cre;Bmpr1a$^{flox-flox}$ mice showed a few foci of cells expressing GSII-positive mucins at the base of the glands. In contrast, *H felis*–infected *Lgr5-Cre;Bmpr1a$^{flox-flox}$* mice showed robust co-expression of mucus neck-cell mucins and IF in cells located at the base of the fundic glands of the mucosa of the lesser curvature. Identical results were observed when the slides were stained with antibodies against TFF2 (Figure 7).

The adhesion molecule and Wnt target CD44 participates in the response of the gastric epithelium to inflammatory stimuli. In addition, CD44 appears to be involved in the pathogenesis of SPEM and to label putative gastric cancer stem cells, suggesting that it might play an important role in the process of inflammation/injury-induced carcinogenesis.[38–43] It also has been shown that alternative mRNA splicing produces *Cd44* variant isoforms, such as *Cd44v9*, which are more specifically expressed in *H pylori* gastritis, SPEM, and in gastric carcinomas.[40,41] Thus, we examined if *H felis*–infected *Lgr5-Cre;Bmpr1a$^{flox-flox}$* mice show perturbations in the expression of both CD44 and of CD44v9. Staining of sections of the lesser curvature of *H felis*–infected *Lgr5-Cre;Bmpr1a$^{flox-flox}$* mice with anti-CD44 antibodies showed robust expression of CD44 in the mucosa of the lesser curvature (Figure 8*A*), with intense staining noted in nests of epithelial cells located at the base of the glands. In contrast, staining of the sections of the lesser curvature of noninfected *Lgr5-Cre;Bmpr1a$^{flox-flox}$* mice and of both infected and noninfected *Lgr5-Cre* mice showed the presence of only a few rare CD44^{+ve} cells at the level of the isthmus and the pits of the gastric glands (Figure 8*A*). Similarly, incubation of sections of the lesser curvature of *H felis*–infected *Lgr5-Cre;Bmpr1a$^{flox-flox}$* mice, but not of noninfected mice, with anti-CD44v9 antibodies showed the presence of extensive staining of cells located at the base of the glands, suggesting that both inflammation and loss of BMP signaling modulate the expression of this splice variant

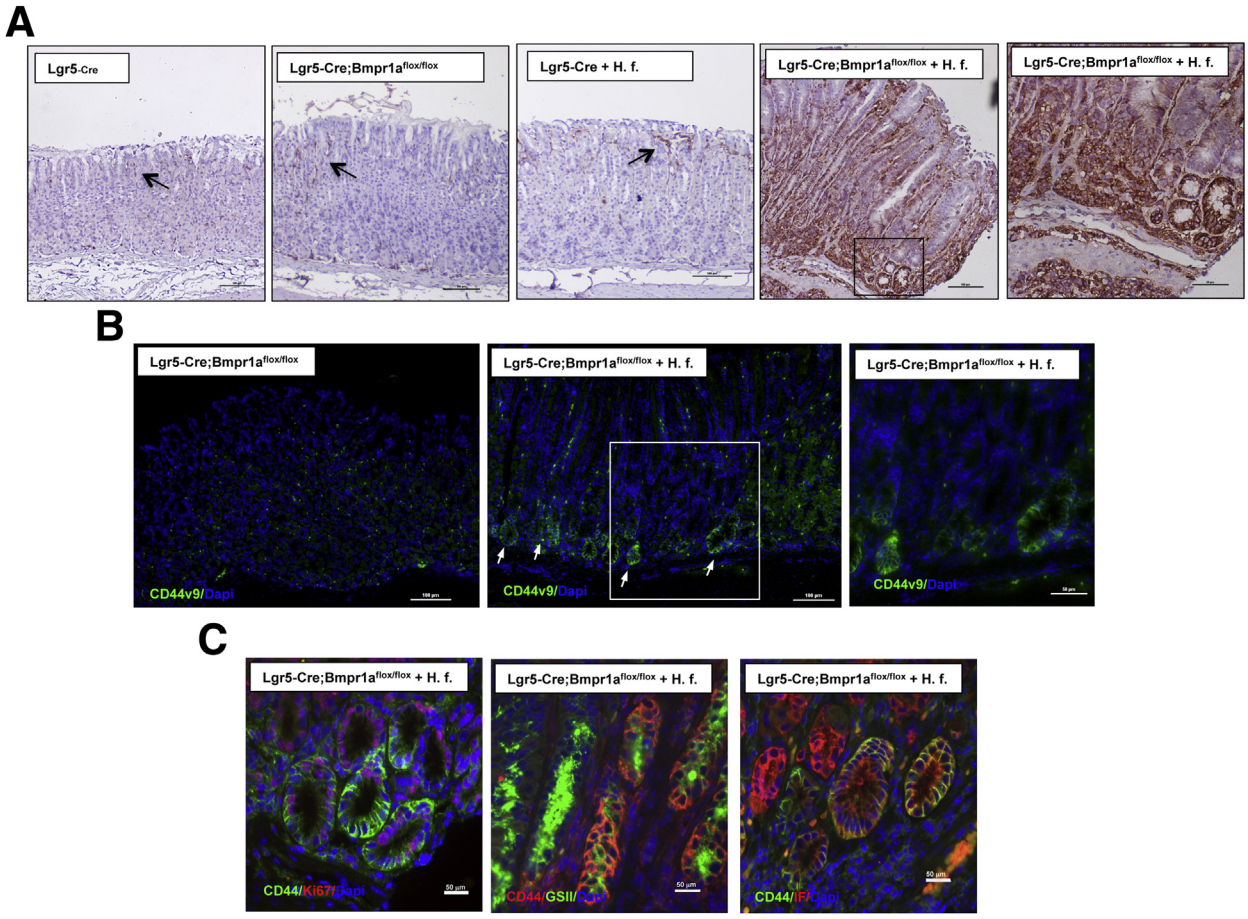

Figure 8. Expression of CD44 in *H felis*–infected *Lgr5-Cre;Bmpr1a*$^{flox\text{-}flox}$ mice. One- to 2-month-old *Lgr5-Cre* mice and *Lgr5-Cre;Bmpr1a*$^{flox\text{-}flox}$ mice were treated with 1 intraperitoneal injection of tamoxifen (0.1 mg/g body weight) and inoculated with *H felis* 2 months after tamoxifen. Animals were analyzed 3 months after inoculation and 5 months after tamoxifen injection. (*A*) Paraffin sections of the lesser curvature of *Lgr5-Cre* and *Lgr5-Cre;Bmpr1a*$^{flox\text{-}flox}$ mice in the presence and absence of *H felis* (H. f.) stained with anti-CD44 primary antibodies and a biotin-conjugated secondary antibody. The magnified window shows intense CD44 staining of epithelial cells in *H felis*–infected *Lgr5-Cre;Bmpr1a*$^{flox\text{-}flox}$ mice. *Scale bar*: 100 μm, 50 μm in the magnified window. *Arrows* point to CD44^{+ve} cells. (*B*) Paraffin sections of the lesser curvature of noninfected and *H felis*–infected *Lgr5-Cre;Bmpr1a*$^{flox\text{-}flox}$ mice stained with anti-CD44v9 primary antibodies and Alexa 488–conjugated secondary antibodies. The magnified window shows CD44v9 staining of epithelial cells at the base of glands in *H felis*–infected *Lgr5-Cre;Bmpr1a*$^{flox\text{-}flox}$ mice. *Scale bar*: 100 μm, 50 μm in the magnified window. *Arrows* point at CD44v9^{+ve} cells. (*C*) Paraffin sections of the lesser curvature of *H felis*–infected *Lgr5-Cre;Bmpr1a*$^{flox\text{-}flox}$ mice stained with anti-CD44 primary antibodies and Alexa 594-conjugated secondary antibodies (*red*) together with Alexa 488–conjugated GSII (*green*), anti-CD44 primary antibodies and Alexa 488–conjugated secondary antibodies (*green*) together with IF antibodies and Alexa 555–conjugated secondary antibodies (*red*) and anti-CD44 primary antibodies and Alexa 488–conjugated secondary antibodies (*green*) together with anti-Ki67 antibodies and Alexa 555–conjugated secondary antibodies (*red*). Similar results were observed in at least 2 other mice in each group. *Scale bar*: 50 μm. DAPI, 4′,6-diamidino-2-phenylindole.

of CD44 (Figure 8*B*). To better define the phenotypic characteristics of CD44-expressing cells in the mucosa of the lesser curvature of *H felis*–infected *Lgr5-Cre;Bmpr1a*$^{flox\text{-}flox}$ mice, we co-stained the sections with anti-CD44 antibodies together with the lectin GSII, IF, and Ki67. As shown in Figure 8*C*, CD44^{+ve} cells, located at the base of the glands, expressed markers of cell proliferation, mucus neck-cell mucins, and IF, suggesting that SPEM can arise in proliferating CD44^{+ve} cells.

By using QRT-PCR assays we also observed increased expression of CD44 mRNA in the gastric mucosa of the lesser curvature of *H felis*–infected *Lgr5-Cre;Bmpr1a*$^{flox\text{-}flox}$ mice when compared with both infected *Lgr5-Cre* mice and noninfected *Lgr5-Cre;Bmpr1a*$^{flox\text{-}flox}$ mice, confirming the notion that inhibition of BMP signaling in Lgr5 cells and the presence of inflammatory stimuli lead to increased CD44 mRNA expression (Figure 9).

In addition to CD44, the oncoprotein c-myc, another Wnt target, has been implicated in gastric carcinogenesis and it has been shown to cooperate with CD44 to regulate gastric cancer growth.[44,45] Accordingly, we performed QRT-PCR assays in which we measured the expression of *c-Myc* mRNA. As shown in Figure 9, *H felis*–infected *Lgr5-Cre;Bmpr1a*$^{flox\text{-}flox}$ mice showed a significant increase in the expression of *c-Myc* when

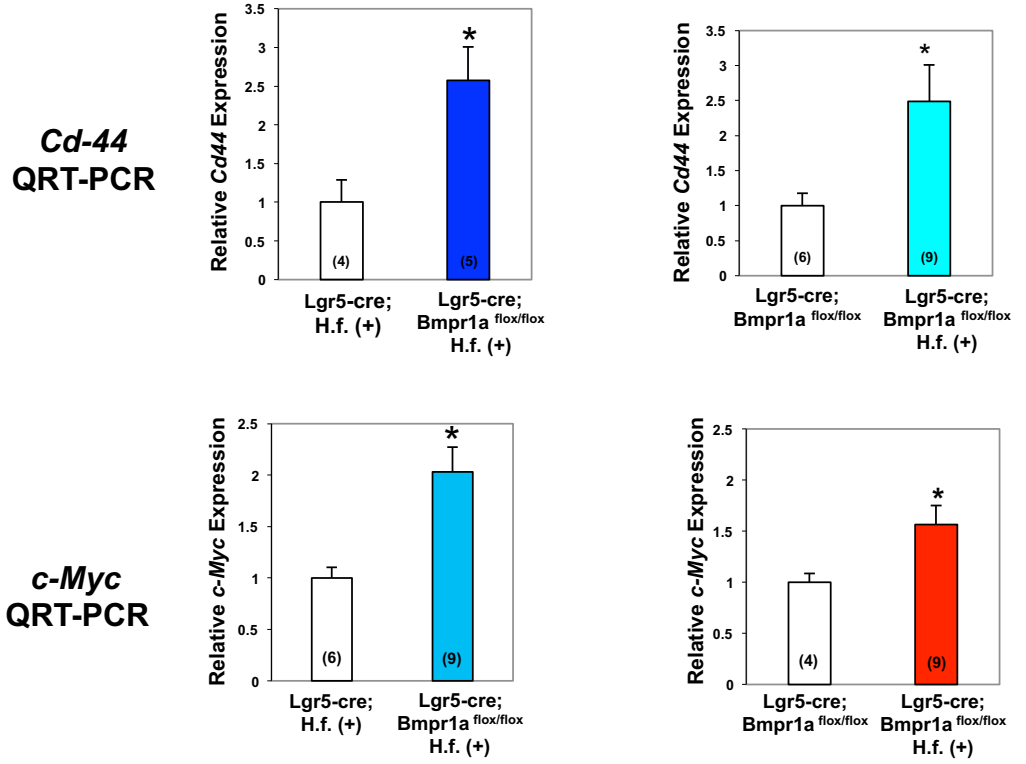

Figure 9. Expression of *Cd44* and *c-Myc* mRNAs in the lesser curvature of *Lgr5-Cre;Bmpr1a*$^{flox\text{-}flox}$ mice. One- to 2-month-old *Lgr5-Cre* mice and *Lgr5-Cre;Bmpr1a*$^{flox\text{-}flox}$ mice were treated with 1 intraperitoneal injection of tamoxifen (0.1 mg/g body weight) and inoculated with *H felis* 2 months after tamoxifen. Animals were analyzed 3 months after inoculation and 5 months after tamoxifen injection. *Cd44* and *c-Myc* mRNA signals in samples of the lesser curvature of *Lgr5-Cre* mice and of *Lgr5-Cre;Bmpr1a*$^{flox\text{-}flox}$ mice in the presence and absence of *H felis* (H. f.) were measured using QRT-PCR. Numbers in parenthesis indicate the number of animals used in each group. $^{*}P < .05$.

compared with both infected *Lgr5-Cre* mice and noninfected *Lgr5-Cre;Bmpr1a*$^{flox\text{-}flox}$ mice, suggesting that inhibition of BMP signaling in Lgr5 cells leads to the development of a pro-oncogenic environment characterized by increased expression of multiple targets of Wnt signaling.

To perform lineage tracing studies in the presence of the BMP inhibitor noggin, we took advantage of *Lgr5-Cre;H*$^{+}$*/K*$^{+}$*-Nog;Rosa26-Tom* mice that express both noggin and tomato in the oxyntic mucosa. As shown in Figure 10*A* a few rare tomato^{+ve} cells could be seen along the lesser curvature of the oxyntic mucosa of both *H felis*–infected and noninfected *Lgr5-Cre* control mice. As shown in the H&E-stained sections, expression of noggin caused significant morphologic changes of the gastric mucosa in agreement with previously published reports,[26,27] but only a modest increase in the number of tomato^{+ve} cells (Figure 10*B*), whereas infection with *H felis* enhanced this effect of noggin, leading to the appearance of robust tomato expression in glandular structures that were located along the lesser curvature of the oxyntic mucosa (Figure 10*C*).

We investigated the cellular lineages that derive from cells with *Lgr5* transcriptional activity in the *H felis*–infected *Lgr5-Cre;H*$^{+}$*/K*$^{+}$*-Nog;Rosa26-Tom* mice. As shown in Figure 11, staining of sections with the lectins Ulex europaeus agglutinin 1 and GSII, molecules that label pit and mucus neck-cell mucins, respectively,[5] and with anti-CD44, anti-CD44v9, and anti-IF antibodies, showed expression of pit and mucus neck-cell markers, CD44, CD44v9, and IF in the tomato-positive cells. These data suggest that pit cell lineages, SPEM, CD44^{+ve}, and CD44v9^{+ve} cells can arise from cells with *Lgr5* transcriptional activity in the presence of inflammatory stimuli and inhibition of BMP signaling. Moreover, as shown in Figure 11, we observed that some of the tomato^{+ve} cells were proliferating because they could be positively stained with anti-BrdU antibodies.

Discussion

In this article, we report a series of novel observations that underscore the importance of BMP signaling in the regulation of gastric epithelial homeostasis. In particular, we present evidence that inhibition of BMP signaling and infection with *H felis* lead to the activation and expansion of Lgr5^{+ve} cells that give rise to metaplastic proliferating lineages that express markers of SPEM.

Although the level of deletion of *Bmpr1a* in Lgr5 cells was not complete, *H felis*–infected *Lgr5-Cre;Bmpr1a*$^{flox\text{-}flox}$ mice showed robust phenotypic changes, suggesting that even partial inhibition of BMP signaling in Lgr5 cells can induce significant aberrations in the normal homeostatic mechanisms of the gastric mucosa. A possible explanation for this finding lies in the observation that Lgr5 cells can express growth-promoting and proinflammatory peptides,[10,38–43] factors known to play an important role in the regulation of cell proliferation and in the response of the gastric mucosa to inflammatory stimuli. It therefore is conceivable that diminished BMP signaling in Lgr5 cells could induce the expression of these molecules leading to

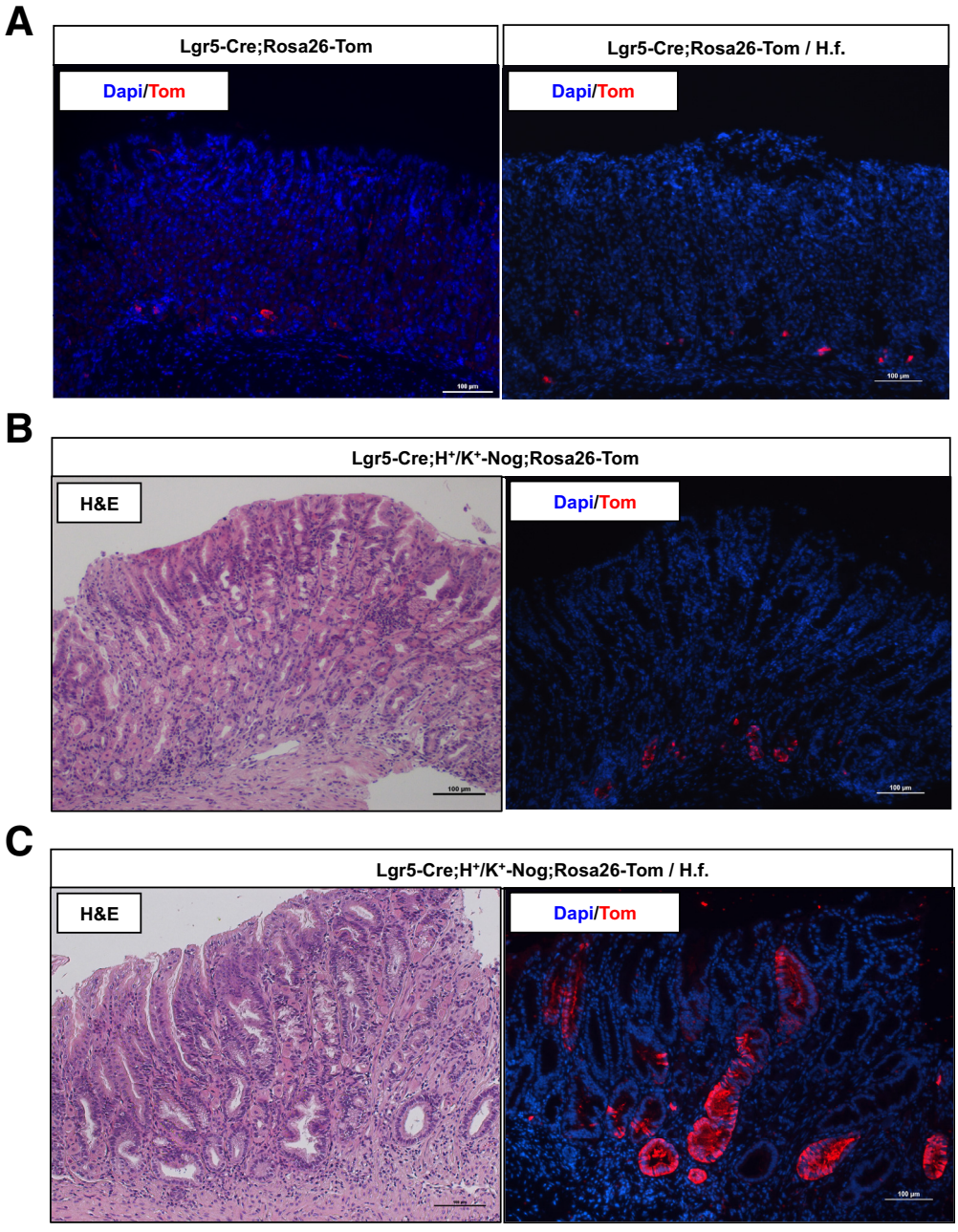

Figure 10. Distribution of tomato-positive cells in *H felis*–infected *Lgr5-Cre;H$^+$/K$^+$-Nog;Rosa26-Tom* mice. One- to 2-month-old *Lgr5-Cre;Rosa26-Tom* mice and *Lgr5-Cre;H$^+$/K$^+$-Nog;-Rosa26-tdTom* mice were treated with 1 intraperitoneal injection of tamoxifen (0.1 mg/g body weight) and inoculated with *H felis* 2 months after tamoxifen. Animals were analyzed 3 months after inoculation and 5 months after tamoxifen injection. Gastric paraffin sections of the lesser curvature of *Lgr5-Cre;Rosa26-Tom* and *Lgr5-Cre;H$^+$/K$^+$-Nog;-Rosa26-tdTom* in the presence and absence of *H felis* (H. f.) were stained with anti-tomato (red fluorescent protein) primary antibodies and Alexa 555–conjugated secondary antibodies. Matching sections of the gastric mucosa of both noninfected and *H felis*–infected *Lgr5-Cre;H$^+$/K$^+$-Nog;Rosa26-tdTom* mice were stained with H&E. Similar results were observed in at least 3 other mice in each group. DAPI, 4′,6-diamidino-2-phenylindole.

broader and more widespread responses that might affect the biological functions not only of Lgr5 cells, but also of other adjacent cell types.

Numerous studies have shown that inflammation, loss of parietal cells, and gastric mucosal injury lead to the reprogramming of a subset of chief cells that undergo profound biological modifications, characterized by the activation of proliferative mechanisms and by the expression of markers of mucus neck-cell differentiation at the base of the glands of the oxyntic mucosa.[5,10,20] These events have been associated with the development of dysplastic changes and gastric carcinogenesis.[5,7–9,20]

Recent reports have shown that in the corpus Lgr5^{+ve} cells express IF, and that these cells represent a subpopulation of chief cells with Lgr5 transcriptional activity.[18,20] Interestingly, elegant lineage tracing studies conducted in *Lgr5-EGFP-IRES-Cre$^{ERT2/+}$;Rosa26R* mice that were treated with either the proinflammatory compound L365 or the protonophore DMP777, which causes ablation of parietal cells without any significant inflammation, did not detect the presence of markers of SPEM in lineages derived from Lgr5 cells located in the lesser curvature.[18] These observations suggest that inflammation and loss of parietal cells, stimuli that can effectively induce SPEM,[5] are not sufficient by

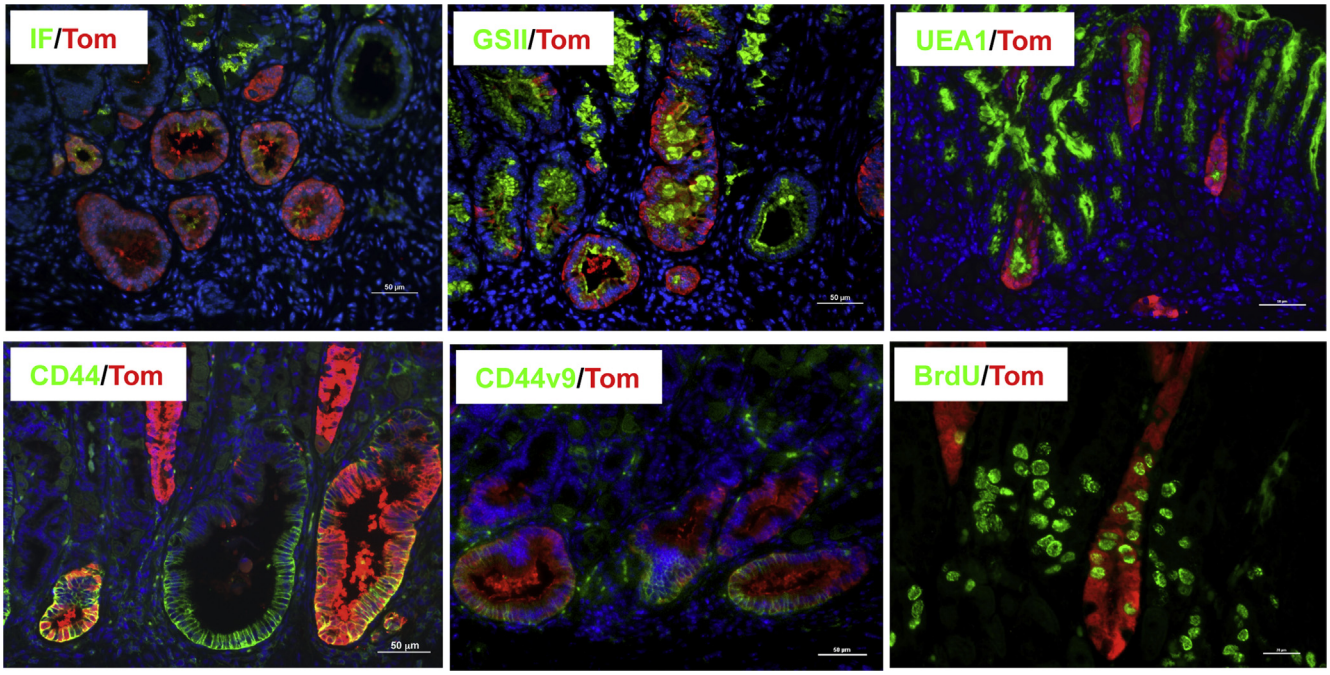

Figure 11. Lineage tracing of cells with *Lgr5* transcriptional activity in *H felis*–infected *Lgr5-Cre;H$^+$/K$^+$-Nog;Rosa26-Tom* mice. 1-2-month old *Lgr5-Cre;H$^+$/K$^+$-Nog;Rosa26-tdTom* mice were treated with one i.p. injection of tamoxifen (0.1 mg/g body weight) and inoculated with *H. felis* two months post tamoxifen. Animals were analyzed 3 months after inoculation, and 5 months after tamoxifen injection. Gastric paraffin sections of the lesser curvature of *H felis*–infected *Lgr5-Cre;H$^+$/K$^+$-Nog;Rosa26-tdTom* mice were stained with anti-tomato (red fluorescent protein) primary antibodies and Alexa 555–conjugated secondary antibodies together with anti-IF antibodies and Alexa 488–conjugated secondary antibodies (IF/Tom), Alexa 488–conjugated GSII (GSII/Tom), Alexa 488–conjugated Ulex europaeus agglutinin 1 (UEA1), anti-CD44 and anti-CD44v9 primary antibodies and Alexa 488–conjugated secondary antibodies (CD44/Tom and CD44v9/Tom), and anti-BrdU primary antibodies and Alexa 488–conjugated secondary antibodies (BrdU/Tom). *Scale bars*: 50 μm. Similar results were observed in at least 5 other *H felis*–infected *Lgr5-Cre;H$^+$/K$^+$-Nog;Rosa26-tdTom* mice except for the experiments with the anti-CD44v9 antibodies that were repeated in 1 other mouse.

themselves to support the development of metaplastic lineages in Lgr5^{+ve} cells.

In our study we observed that either infection with *H felis* or inhibition of BMP signaling by themselves caused only small changes in the number and fate of Lgr5^{+ve} cells. However, infection with *H felis* in the presence of inhibition of BMP signaling led to robust aberrations in the normal homeostatic mechanisms of the gastric epithelium characterized by the emergence of SPEM in glands derived from cells with *Lgr5* transcriptional activity located along the lesser curvature of the oxyntic mucosa. It is possible that some of these changes could have been caused by the heightened level of inflammation caused by *H felis* in the presence of loss of BMP signaling, a mechanism that we previously showed has anti-inflammatory effects.[27] However, the observation that neither L365 nor *H felis* by themselves were able to induce the emergence of SPEM in Lgr5 progenitors[18] suggests that BMP signaling has additional, specific actions on the physiological mechanisms that regulate the proliferation and differentiation of gastric epithelial cells. In support of this hypothesis, transgenic mice that express the BMP signaling inhibitor noggin in the gastric epithelium develop epithelial hyperproliferation and extensive SPEM in the context of only minimal inflammatory changes.[26,27]

An important factor that should be considered in the interpretation of our results is that in this study we used the *Lgr5-EGFP-ires-CreERT2* (*Lgr5-Cre*) mouse model in which *EGFP* and *Cre* were expressed only in the antrum and along the lesser curvature of the oxyntic mucosa.[11] It is therefore conceivable that the changes observed in our studies could have been detected in more extensive areas of the corpus if we had used the *Lgr5-2A-CreERT2* mouse, a biological system[20] that allows an unrestricted expression of the transgene in all segments of the gastric mucosa.

The intracellular mechanisms responsible for the development of SPEM have been only partially characterized. Recent reports have indicated that activation of the Ras/extracellular signal–regulated kinase (ERK) kinase signal transduction pathway in chief cells leads to SPEM, suggesting that this signaling mechanism plays an important role in the biological processes that cause the emergence of this type of metaplasia.[20,46] Interestingly, in a series of previously published studies we observed that inhibition of BMP signaling leads to enhanced activation of the ERKs and to increased growth factor gene expression in the gastric mucosa.[26] We also reported that BMP-4, a member of the BMP family of regulatory peptides, inhibits growth factor–stimulated ERK2 activation in primary cultures of canine gastric epithelial cells,[47] confirming the notion that

the BMP signal transduction pathway restrains the induction of growth factor signaling in the stomach. On the basis of these observations it is conceivable to speculate that inhibition of BMP signaling in Lgr5 cells could remove an inhibitory break on ERK activation, leading to the induction of a series of intracellular events that ultimately could lead to the development of SPEM and to the stimulation of proliferative mechanisms. In support of this observation recent studies have shown that induction of Ras activation in *Lgr5*-expressing chief cells can lead to the development of metaplasia and neoplasia.[20,46]

We reported that diminished expression of *Bmpr1a* and noggin cause increased expression of CD44 in the gastric epithelium of the lesser curvature and in epithelial cells derived from $Lgr5^{+ve}$ cells. CD44 has been implicated in the pathogenesis of inflammation, SPEM, and in the process of gastric carcinogenesis because *Cd44*-expressing cells isolated from gastric tumors behave as gastric cancer stem cells.[38–43] Studies also have shown that induction of mitogen-activated protein kinase/ERK signaling leads to increased expression of CD44,[38] and to the activation of STAT3, a pro-oncogenic molecule that has been linked to gastric carcinogenesis.[48,49] Elegant biochemical experiments have shown that CD44 physically interacts with phosphorylated STAT3 and that the CD44/phosphorylated STAT3 complex is necessary for induction of cell proliferation.[38] Because we previously reported that *H pylori*–infected noggin transgenic mice show enhanced activation of STAT3,[27] it is possible that inhibition of BMP signaling in Lgr5 cells could activate a biochemical cascade that links the ERKs to CD44 and STAT3, leading to stimulation of cell proliferation and to the development of metaplastic changes of the gastric mucosa.

The expression of CD44 in pathologic states of the stomach is complex, and there are some isoforms of CD44, such as CD44v6 and CD44v9, that have been more specifically linked to gastric inflammation and neoplasia.[40,41] Our experiments confirm the involvement of CD44v9 in the phenotypic changes observed in *Lgr5-Cre;Bmpr1a*$^{flox\text{-}flox}$ mice. Future studies will be needed to analyze in more detail the CD44 isoforms that specifically are linked to altered BMP signaling and to Lgr5 cell fate during *Helicobacter*-induced inflammation.

In our study we also observed a significant increase in the expression of *c-Myc*, a Wnt target that has been implicated in gastric carcinogenesis and that appears to cooperate with CD44 in the regulation of gastric cancer growth.[44,45] Thus, inhibition of BMP signaling and activation of inflammatory mechanisms appear to lead to the induction of multiple Wnt targets and to the development of a pro-oncogenic environment.

In conclusion, we have shown that inflammation and inhibition of BMP signaling lead to the activation of cells with *Lgr5* transcriptional activity that give rise to dysplastic, proliferating lineages that express markers of both mucus neck and zymogenic cell differentiation. These findings underscore the importance of BMP signaling in the regulation of gastric inflammation and epithelial homeostasis, providing new clues for a better understanding of the pathophysiological mechanisms that lead to the development of both dysplastic and neoplastic lesions in the stomach.

References

1. Peek RM Jr. IV. Helicobacter pylori strain-specific activation of signal transduction cascades related to gastric inflammation. Am J Physiol Gastrointest Liver Physiol 2001;280:G525–G530.
2. Nomura S, Baxter T, Yamaguchi H, Leys C, Vartapetian AB, Fox JG, Lee JR, Wang TC, Goldenring JR. Spasmolytic polypeptide expressing metaplasia to preneoplasia in H. felis-infected mice. Gastroenterology 2004;127:582–594.
3. Zavros Y, Eaton KA, Kang W, Rathinavelu S, Katukuri V, Kao JY, Samuelson LC, Merchant JL. Chronic gastritis in the hypochlorhydric gastrin-deficient mouse progresses to adenocarcinoma. Oncogene 2005; 24:2354–2366.
4. Peek RM, Fiske C, Wilson KT. Role of innate immunity in Helicobacter pylori-induced gastric malignancy. Physiol Rev 2010;90:831–858.
5. Petersen CP, Mills JC, Goldenring JR. Murine models of gastric corpus preneoplasia. Cell Mol Gastroenterol Hepatol 2017;3:11–26.
6. Levi E, Sochacki P, Khoury N, Patel BB, Majumdar AP. Cancer stem cells in Helicobacter pylori infection and aging: implications for gastric carcinogenesis. World J Gastrointest Pathophysiol 2014;5:366–372.
7. Halldorsdottir AM, Sigurdardottir M, Jonasson JG, Oddsdóttir M, Magnússon J, Lee JR, Goldenring JR. Spasmolytic polypeptide expressing metaplasia (SPEM) associated with gastric cancer in island. Dig Dis Sci 2003;48:431–441.
8. Goldenring JR, Nam KT, Wang TC, Mills JC, Wright NA. Spasmolytic polypeptide-expressing metaplasia and intestinal metaplasia: time for reevaluation of metaplasias and the origins of gastric cancer. Gastroenterology 2010; 138:2207–2210.
9. Noto JM, Peek RM Jr. Gastric-to-intestinal transdifferentiation and cancer. Proc Natl Acad Sci U S A 2012;109:20173–20174.
10. Nam KT, Lee H-J, Sousa JF, Weis VG, O'Neal RL, Finke PE, Romero-Gallo J, Shi G, Mills JC, Peek RM Jr, Konieczny SF, Goldenring JR. Mature chief cells are cryptic progenitors for metaplasia in the stomach. Gastroenterology 2010;139:2028–2037.
11. Barker N, Meritexell H, Kujala P, van de Wetering M, Snippert HJ, van Es JH, Sato T, Stange DE, Begthel H, van den Born M, Danenberg E, van den Brink S, Korving J, Abo A, Peters PJ, Wright N, Poulsom R, Clevers H. Lgr5+ve stem cells drive self-renewal in the stomach and build long-lived gastric units in vitro. Cell Stem Cell 2010;6:25–36.
12. Arnold K, Sarkar A, Myram MA, Polo JM, Bronson R, Sengupta S, Seandel M, Geijsen N, Hochedlinger K. $Sox2^{+}$ adult stem/progenitor cells are important for tissue regeneration and survival of mice. Cell Stem Cell 2011;9:317–329.
13. Mills JC, Shivdasani RA. Gastric epithelial stem cells. Gastroenterology 2011;140:412–424.

14. Qiao XT, Gumucio DL. Current molecular markers for gastric progenitor cells and gastric cancer stem cells. J Gastroenterol 2011;46:855–865.
15. Stange DE, Koo BK, Huch M, Sibbel G, Basak O, Lyubimova A, Kujala P, Bartfeld S, Koster J, Geahlen JH, Peters PJ, van Es JH, van de Wetering M, Mills JC, Clevers H. Differentiated Troy+ chief cells act as reserve stem cells to generate all lineages of the stomach epithelium. Cell 2013;155:357–368.
16. Hayakawa Y, Ariyama H, Stancikova J, Sakitani K, Asfaha S, Renz BW, Dubeykovskaya ZA, Shibata W, Wang H, Westphalen CB, Chen X, Takemoto Y, Kim W, Khurana SS, Tailor Y, Nagar K, Tomita H, Hara A, Sepulveda AR, Setlik W, Gershon MD, Saha S, Ding L, Shen Z, Fox JG, Friedman RA, Konieczny SF, Worthley DL, Korinek V, Wang TC. Mist1 expressing gastric stem cells maintain the normal and neoplastic gastric epithelium and are supported by a perivascular stem cell niche. Cancer Cell 2015;28:800–814.
17. Matsuo J, Kimura S, Yamamura A, Koh CP, Hossain MZ, Heng DL, Kohu K, Voon DC, Hiai H, Unno M, So JB, Zhu F, Srivastava S, Teh M, Yeoh KG, Osato M, Ito Y. Identification of stem cells in the epithelium of the stomach corpus and antrum of mice. Gastroenterology 2017;152:218–223.
18. Nam KT, O'Neal RL, Coffey RJ, Finke PE, Barker N, Goldenring JR. Spasmolytic polypeptide-expressing metaplasia (SPEM) in the gastric oxyntic mucosa does not arise from Lgr5-expressing cells. Gut 2012; 61:1678–1685.
19. Ajani JA, Barthel JS, Bekaii-Saab T, Bentrem DJ, D'Amico TA, Das P, Denlinger C, Fuchs CS, Gerdes H, Hayman JA, Hazard L, Hofstetter WL, Ilson DH, Keswani RN, Kleinberg LR, Korn M, Meredith K, Mulcahy MF, Orringer MB, Osarogiagbon RU, Posey JA, Sasson AR, Scott WJ, Shibata S, Strong VE, Washington MK, Willett C, Wood DE, Wright CD, Yang G. NCCN Gastric Cancer Panel. J Natl Compr Canc Netw 2010;8:378–409.
20. Leushacke M, Tan SH, Wong A, Swathi Y, Hajamohideen A, Tan LT, Goh J, Wong E, Denil SLIJ, Murakami K, Barker N. *Lgr5*-expressing chief cells drive epithelial regeneration and cancer in the oxyntic stomach. Nat Cell Biol 2017;19:774–786.
21. Jang BG, Lee BL, Kim WH. Distribution of LGR5+ cells and associated implications during the early stage of gastric tumorigenesis. PLoS One 2013;8:e82390.
22. Li X-B, Yang G, Zhu L, Tang YL, Zhang C, Ju Z, Yang X, Teng Y. Gastric Lgr5^{+}stem cells are the cellular origin of invasive intestinal-type gastric cancer in mice. Cell Res 2016;26:838–849.
23. Sigal M, Rothenberg ME, Logan CY, Lee JY, Honaker RW, Cooper RL, Passarelli B, Camorlinga M, Bouley DM, Alvarez G, Nusse R, Torres J, Amieva MR. Helicobacter pylori activates and expands Lgr5(+) stem cells through direct colonization of the gastric glands. Gastroenterology 2015;148:1392–1404.
24. Brazil DP, Church RH, Surae S, Godson C, Martin F. BMP signaling: agony and antagony in the family. Trends Cell Biol 2015;25:249–264.
25. Todisco A. Regulation of gastric metaplasia, dysplasia, and neoplasia by bone morphogenetic protein signaling. Cell Mol Gastroenterol Hepatol 2017;3:339–347.
26. Shinohara M, Mao M, Keeley TM, El-Zaatari M, Lee HJ, Eaton KA, Samuelson LC, Merchant JL, Goldenring JR, Todisco A. Bone morphogenetic protein signaling regulates gastric epithelial cell development and proliferation in mice. Gastroenterology 2010;139:2050–2060.
27. Takabayashi H, Shinohara M, Mao M, Phaosawasdi P, El-Zaatari M, Zhang M, Ji T, Eaton KA, Dang D, Kao J, Todisco A. Anti-inflammatory activity of bone morphogenetic protein signaling pathways in stomachs of mice. Gastroenterology 2014;147:396–406.
28. Uhlén M, Fagerberg L, Hallström BM, Lindskog C, Oksvold P, Mardinoglu A, Sivertsson Å Kampf C, Sjöstedt E, Asplund A, Olsson I, Edlund K, Lundberg E, Navani S, Szigyarto CA, Odeberg J, Djureinovic D, Takanen JO, Hober S, Alm T, Edqvist PH, Berling H, Tegel H, Mulder J, Rockberg J, Nilsson P, Schwenk JM, Hamsten M, von Feilitzen K, Forsberg M, Persson L, Johansson F, Zwahlen M, von Heijne G, Nielsen J, Pontén F. Tissue-based map of the human proteome. Science 2015;347:1260419.
29. Mishina Y, Hanks MC, Miura S, Tallquist MD, Behringer RR. Generation of Bmpr/Alk3 conditional knockout mice. Genesis 2002;32:69–72.
30. Eaton KA, Benson LH, Haeger J, Gray BM. Role of transcription factor T-bet expression by CD4+ cells in gastritis due to *Helicobacter pylori* in mice. Infect Immun 2006;74:4673–4684.
31. Demitrack ES, Gifford GB, Keeley TM, Carulli AJ, VanDussen KL, Thomas D, Giordano TJ, Liu Z, Kopan R, Samuelson LC. Notch signaling regulates gastric antral LGR5 stem cell function. EMBO J 2015;34:2522–2536.
32. Eaton KA, Danon SJ, Krakowka S, Weisbrode SE. A reproducible scoring system for quantification of histologic lesions of inflammatory disease in mouse gastric epithelium. Comp Med 2007;57:57–65.32.
33. Schindelin J, Arganda-Carreras I, Frise E, Kaynig V, Longair M, Pietzsch T, Preibisch S, Rueden C, Saalfeld S, Schmid B, Tinevez JY, White DJ, Hartenstein V, Eliceiri K, Tomancak P, Cardona A. Fiji: an open-source platform for biological-image analysis. Nat Methods 2012;28; 9:676–682.
34. Locklin RM, Riggs BL, Hicok KC, Horton HF, Byrne MC, Khosla S. Assessment of gene regulation by bone morphogenetic protein 2 in human marrow stromal cells using gene array technology. J Bone Miner Res 2001; 16:2192–2204.
35. Miyazono K, Maeda S, Imamura T. BMP receptor signaling: transcriptional targets, regulation of signals, and signaling cross-talk. Cytokine Growth Factor Rev 2005;16:251–263.
36. Bonilla-Claudio M, Wang J, Bai Y, Klysik E, Selever J, Martin JF. Bmp signaling regulates a dose-dependent transcriptional program to control facial skeletal development. Development 2012;139:709–719.
37. Zhang S, Moss SF. Rodent models of *Helicobacter* infection, inflammation and disease. Methods Mol Biol 2012;921:89–98.

38. Khurana SS, Riehl TE, Moore BD, Fassan M, Rugge M, Romero-Gallo J, Noto J, Peek RM Jr, Stenson WF, Mills JC. The hyaluronic acid receptor CD44 coordinates normal and metaplastic gastric epithelial progenitor cell proliferation. J Biol Chem 2013;288:16085–16097.
39. Ishimoto T, Izumi D, Watanabe M, Yoshida N, Hidaka K, Miyake K, Sugihara H, Sawayama H, Imamura Y, Iwatsuki M, Iwagami S, Baba Y, Horlad H, Komohara Y, Takeya M, Baba H. Chronic inflammation with Helicobacter pylori infection is implicated in CD44 overexpression through miR-328 suppression in the gastric mucosa. J Gastroenterol 2015;50:751–757.
40. Wada T, Ishimoto T, Seishima R, Tsuchihashi K, Yoshikawa M, Oshima H, Oshima M, Masuko T, Wright NA, Furuhashi S, Hirashima K, Baba H, Kitagawa Y, Saya H, Nagano O. Functional role of CD44v-xCT system in the development of spasmolytic polypeptide-expressing metaplasia. Cancer Sci 2013;104:1323–1329.
41. Zavros Y. Initiation and maintenance of gastric cancer: a focus on CD44 variant isoforms and cancer stem cells. Cell Mol Gastroenterol Hepatol 2017;4:55–63.
42. Seishima R, Wada T, Tsuchihashi K, Okazaki S, Yoshikawa M, Oshima H, Oshima M, Sato T, Hasegawa H, Kitagawa Y, Goldenring JR, Saya H, Nagano O. Ink4a/Arf-dependent loss of parietal cells induced by oxidative stress promotes CD44-dependent gastric tumorigenesis. Cancer Prev Res (Phila) 2015;8:492–501.
43. Takaishi S, Okumura T, Tu S, Wang SS, Shibata W, Vigneshwaran R, Gordon SA, Shimada Y, Wang TC. Identification of gastric cancer stem cells using cell surface makers CD44. Stem Cells 2009;27:1006–1020.
44. Wilkins JA, Sansom OJ. Is a critical mediator of the phenotypes of *Apc* loss in the intestine. Cancer Res 2008;68:4963–4966.
45. Park J, Kim SY, Kim HJ, Kim KM, Choi EY, Kang MS. A reciprocal regulatory circuit between CD44 and FGFR2 via c-myc controls gastric cancer cell growth. Oncotarget 2016;7:28670–28683.
46. Choi E, Hendley AM, Bailey JM, Leach SD, Goldenring JR. Expression of activated Ras in gastric chief cells of mice leads to the full spectrum of metaplastic lineage transitions. Gastroenterology 2016;150:918–930.
47. Nitsche H, Ramamoorthy S, Sareban M, Pausawasdi N, Todisco A. Functional role of bone morphogenetic protein-4 in isolated canine parietal cells. Am J Physiol Gastrointest Liver Physiol 2007;293:G607–G614.
48. Ernst M, Najdovska M, Grail D, Lundgren-May T, Buchert M, Tye H, Matthews VB, Armes J, Bhathal PS, Hughes NR, Marcusson EG, Karras JG, Na S, Sedgwick JD, Hertzog PJ, Jenkins BJ. STAT3 and STAT1 mediate IL-11 dependent and inflammation-associated gastric tumurogenesis in gp130 receptor mutant mice. J Clin Invest 2008;118:1727–1738.
49. Li N, Grivennikov SI, Karin M. The unholy trinity: inflammation, cytokines, and STAT3 shape the cancer microenvironment. Cancer Cell 2011;19:429–431.

Received March 25, 2017. Accepted January 9, 2018.

Correspondence
Address correspondence to: Andrea Todisco, MD, 6520 Medical Science Research Building I, Ann Arbor, Michigan 48109-0682. e-mail: atodisco@umich.edu; fax: (734) 763-2535.

Acknowledgments
The authors thank Kathy McClinchey for technical assistance and the University of Michigan Flow Cytometry Core for technical assistance with cell sorting.

Author contributions
Wei Ye and Hidehiko Takabayashi were responsible for the study concept and design, acquisition of data, analysis and interpretation of data, critical revision of the manuscript, and statistical analysis; Maria Mao and Yitian Yang were responsible for the acquisition of data, analysis and interpretation of data, technical support, and statistical analysis; Elise S. Hibdon was responsible for the acquisition of data, analysis and interpretation of data, and critical revision of the manuscript for important intellectual content; Linda C. Samuelson was responsible for the analysis and interpretation of data and critical revision of the manuscript for important intellectual content; Kathryn A. Eaton was responsible for the acquisition, analysis and interpretation of data, and critical revision of the manuscript for important intellectual content; and Andrea Todisco was responsible for the study concept and design, acquisition of data, analysis and interpretation of data, critical revision of the manuscript for important intellectual content, statistical analysis, obtained funding, study supervision, and writing the manuscript.

Conflicts of interest
The authors disclose no conflicts.

Funding
This work was supported by National Institute of Diabetes and Digestive and Kidney Diseases grants RO1DK083373 and R56DK116617 (A.T.), by the University of Michigan Gastrointestinal Peptide Research Center (P30-DK-34933), by the University of Michigan Comprehensive Cancer Center John S. and Suzanne C. Munn Cancer Fund (A.T.), and by the Funderburg Award in Gastric Biology Related to Cancer from the Foundation for Digestive Health and Nutrition (A.T.).